

2011

## Folding and Base Pairing of a Fibrinogen Specific DNA Aptamer

Christopher J. Hamilton

*Georgia State University*, [chamilton6@student.gsu.edu](mailto:chamilton6@student.gsu.edu)

Markus W. Germann

*Georgia State University*, [mwg@gsu.edu](mailto:mwg@gsu.edu)

Follow this and additional works at: <https://scholarworks.wm.edu/caaurj>

---

### Recommended Citation

Hamilton, Christopher J. and Germann, Markus W. (2011) "Folding and Base Pairing of a Fibrinogen Specific DNA Aptamer," *Colonial Academic Alliance Undergraduate Research Journal*: Vol. 2 , Article 11.

Available at: <https://scholarworks.wm.edu/caaurj/vol2/iss1/11>

This Article is brought to you for free and open access by the Journals at W&M ScholarWorks. It has been accepted for inclusion in Colonial Academic Alliance Undergraduate Research Journal by an authorized editor of W&M ScholarWorks. For more information, please contact [scholarworks@wm.edu](mailto:scholarworks@wm.edu).

---

# Folding and Base Pairing of a Fibrinogen Specific DNA Aptamer

## **Cover Page Note**

Acknowledgements We thank Dr. B. Wang for the generous gift of the phosphoramidites. C.J.H. was supported from a Molecular Basis of Disease fellowship and University Scholar Assistantship program from Georgia State.

## Introduction

Aptamers are nucleic acid or peptide molecules that bind to a specific target. DNA and RNA aptamers were first developed independently in three laboratories in 1990 using *in vitro* selection or SELEX (Systematic Evolution of Ligands by Exponential Enrichment) to target T4 DNA polymerase or thrombin<sup>1, 2, 3</sup>.

The process of SELEX spawns DNA or RNA sequences with constant primer regions flanking a variable nucleotide portion until the desired target affinity is achieved (Figure 1). Nucleic acids that either do not bind or do so only weakly are discarded by a wash step. The sequences that bind more strongly are subsequently eluted and enriched to generate a new cohort of binding sequences with higher affinities. The binding/selection/enhancement cycle is repeated with more stringent wash steps until aptamers with the desired affinity are obtained.

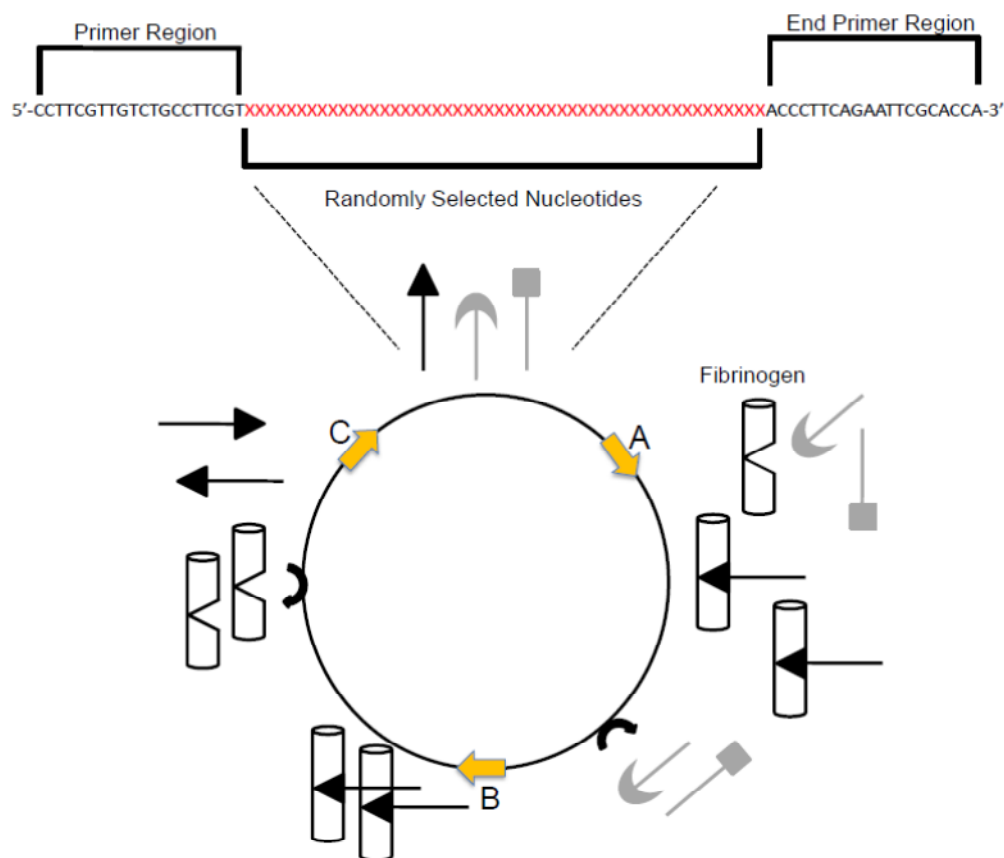


**Figure 1:** SELEX model for selection of fibrinogen. Randomly generated nucleotides are synthesized and introduced to the target molecule, fibrinogen. DNA sequences that do not bind or do so weakly are removed via a wash step (A). The binding sequences are separated from their target molecules and isolated (B). Binding sequences are amplified and undergo more stringent binding parameters until an aptamer is selected (C).

Although aptamers have only recently been developed, many applications have been developed. Aptamers are extremely versatile and can target small organic molecules, proteins, other nucleic acids and even cells. In addition to a wide range of targets, aptamers are able to bind their target with a high affinity, often in the pM-nM range while maintaining a high degree of discrimination<sup>4</sup>. For example, an aptamer specific for theophylline binds caffeine, which differs by a single methyl group, 10,000x more weakly.<sup>4</sup>

These characteristics encouraged the development of aptamers as inhibitors, detectors and macro-molecular drugs<sup>5,6,7</sup>. For example, an aptamer was employed as the stationary phase in novel L-Selectin chromatographic columns<sup>6</sup>. In addition to attachment to a matrix, aptamers can also be further chemically modified to introduce additional chemical diversity or to incorporate task specific moieties. For example; an aptamer can be biotinylated for immobilizations or a fluorescent moiety can be introduced to facilitate its detection<sup>7</sup>. The high binding affinity and selectivity makes them attractive candidates as macromolecular drugs. Jeon et al. developed an aptamer that is specific to the glycoprotein hemagglutinin of the influenza virus, which is responsible for the virus binding to its host cell<sup>5</sup>. The results of that study showed that this construct is capable of both prevention and treatment of the influenza virus *in vivo*. DNA and RNA are only slightly immunogenic and are readily degraded by nucleases; however, these disadvantages can be modulated or prevented by chemical modifications<sup>8,9</sup>.

Currently, there is one aptamer based therapeutic drug approved by the FDA. This drug, named Macugen, was designed to treat age-related macular degeneration by targeting vascular endothelial growth factor, a signal protein responsible for angiogenesis. The drug is pegylated, which further reduces its immunogenicity and also increases its bioavailability.<sup>10</sup>

To understand the binding with the target and possibly improve it, knowledge of the structural details is desired. Aptamers can be quite large, but only specific regions might be actually responsible for binding, thus it may be possible to remove non essential portions while retaining specificity. For example, comparing the binding affinities of a full-length aptamer (218 nucleotides) to a truncated form (149 nucleotides) resulted in  $K_D$ s of 31nM and 21nM respectively<sup>11</sup>. Further, NMR structural studies on a thrombin binding oligonucleotide showed that the small 15 nucleotide sequence is highly compact and forms a quadruplex structure in solution<sup>12</sup>.

This study investigates the structure of a DNA aptamer (Ap90), specific for the glycoprotein fibrinogen by gel electrophoresis, structure prediction and NMR spectroscopy. This aptamer was previously shown to bind fibrinogen with a  $K_D$  of 64 nM, a corresponding sequence containing boronic acid modified thymidines binds the target even better with a  $K_D$  of 6.4 nM<sup>13</sup>. The binding of an aptamer to fibrinogen will likely inhibit its function and is therefore potentially a



**Denaturing Polyacrylamide Gel Electrophoresis (PAGE):** Gel Electrophoresis was used to assess the purity of the synthesized DNA. After synthesis, 0.2 OD<sub>260nm</sub> (108ng) of each synthesized DNA sequence (15µL in 1x TBE, 90% formamide) was heated to 90 °C for 5 minutes and applied to a 10% denaturing PAGE 1mm gel containing 8M urea. Bands corresponding to DNA oligomers were visualized by UV shadowing using a TLC plate with UV indicator and a handheld UV lamp. Both Su18 and Su32 were of sufficient purity but Ap90 showed the presence of some failure sequences that would hamper the analysis. To purify the full length aptamer, 100 OD<sub>260nm</sub> (3.6mg) of the crude synthesis (1mL in 1x TBE, 90% formamide) was loaded on a 195x160x3mm 15% denaturing PAGE containing 8M urea. A total of 2 gels were prepared. After running the gel the DNA bands were visualized by UV shadowing. The top band corresponding to full length aptamer was excised with a scalpel and extracted 3 times with 25mL 1xTBE buffer on a shaker overnight. The collected supernatants were centrifuged and lyophilized. The sample was then resuspended in deionized H<sub>2</sub>O and desalted using Hitrap desalting columns as described previously and subsequently quantified. Following purification the overall yield of Ap90 from 2x1µM synthesis was 117 OD<sub>260nm</sub> (4.2mg).

**Native PAGE:** 0.02 OD<sub>260</sub> (~108ng) of full length aptamer Ap90 (15µL in tris-borate-magnesium chloride running buffer (TBM), 40% sucrose) was analyzed on a 12% native gel to probe the structure of the non-denatured aptamer by comparing its mobility to that of various length 0.01OD<sub>260</sub> (~59ng) single stranded oligomers ranging from 10 to 90 nucleotides in length. The gel was stained with SYBR green II (Molecular Probes) on a shaker for 30 minutes, following the protocol from the manufacturer. The gel was then visualized on a GE Typhoon 9400 at an excitation wavelength of 532nm. The single stranded sequences that Ap90 was compared to are listed below.

90-mer: dCAAATTATCTTTTCATCCACACATATTCTATCT  
 AATTCCTCATCCTACTTATTTCTCTCCTCCCAC  
 CATTATCTATTAACATTCCACCAT  
 50-mer: dTACGACTCTACGATCAGCATAATCATCCA  
 TTTACTCTGTTACTGTATCCG  
 30-mer: dTTTTTCATGACCGTACGTCTCGAACTTTTT  
 18-mer: dGCAAGTCCAGCCAAATGC  
 10-mer: dCCGTACGTCT

**Secondary Structure Prediction Using the Software MFOLD:** The parameters for MFOLD were set to default which allowed for a broad variety of predicted

secondary structures<sup>16</sup>. The following settings were used: temperature was set to 37°C. The salt conditions were at 1.0M NaCl; percent suboptimality, the percentage range from the minimum free energy, was set to 5; upper bound, the factor that determines how different the secondary structures should be relative to one another, was set to 50; the max distance between base pairs was set to no limit.

**NMR experiments:** All experiments were recorded on a Bruker Avance 500MHz NMR using a 5mm triple resonance TBI probe. NMR samples of 350µL were prepared in 90% H<sub>2</sub>O, 10% D<sub>2</sub>O, 1.4mM EDTA, in NaCl, in either sodium phosphate (pH 7.0) or tris (tris(hydroxymethyl)aminomethane) (pH 7.3) buffers. All samples were measured in 5mm Shigemi NMR tubes at temperatures ranging from 5° C to 55° C. A Jump and Return pulse sequence was used for solvent suppression and to detect the imino protons<sup>17</sup>. The delay between the phase shifted pulses was set to 50µs for optimal excitation of the imino proton region. The relaxation delay was set to 0.1s with an acquisition time of 0.3s for most of the experiments. The number of scans depended on the sample and experiments and ranged from 256 to 32k. For samples containing 1M sucrose, the hard pulses in the jump and return pulse sequence were replaced by 90° shaped pulses (Eburp with a duration of 1.8 ms centered on the imino proton region).

## **Results**

**Synthesis and Purification:** Following synthesis and deprotection, all DNA oligonucleotides were analyzed by denaturing gel electrophoresis. The aptamer Ap90 showed the presence of some failure sequences and was therefore purified by gel extraction. All oligonucleotides showed single bands on a denaturing gel and were desalted prior to use.

**Folding:** Native gel electrophoresis is a convenient method to assess folding of nucleic acids. Ap90 exhibits a mobility that is drastically different from a single stranded 90-mer. Ap90 appears as a smear that is centered between 30- and 50-mer markers. Under denaturing conditions Ap90 migrates as a single band, consequently the large range in mobilities observed in the native gel is not due to impurities. Instead, the width of the band suggests that the aptamer adopts multiple conformations that have different electrophoretic mobilities (Figure 2).

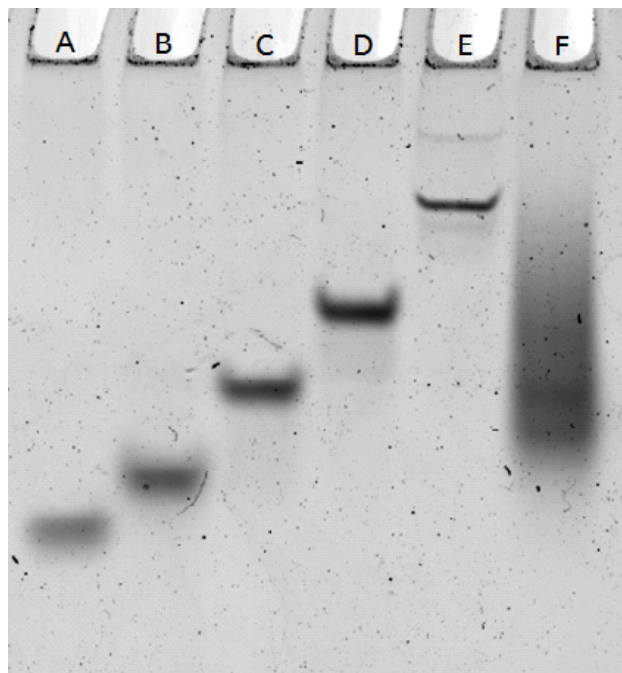


**Figure 2:** 12% Native PAGE to observe mobilities of Ap90. Ap90 is compared to single stranded oligomers of various lengths. The lanes were loaded from the smallest to the largest sequences with Lane A-E containing the 10-mer, 18-mer, 30-mer, 50-mer, and the 90-mer respectively. Lane F contains the aptamer Ap90. The smear in lane F encompassing a large range of DNA sizes (~90 nucleotides - ~30 nucleotides) indicates that the aptamer has multiple conformations.

**Structure prediction:** Nucleic acid structure prediction algorithms are useful to gain insight in possible secondary structure formation. MFOLD generates potential low energy structures; the software takes hairpin loops and other structural perturbations into account when folding the molecule<sup>16</sup>. For the aptamer many possible secondary structures are predicted that all generate a similar predicted energy (Figure 3). It is noteworthy that despite the large variety of secondary structures, most of them had ~11 base pairs indicating that the aptamer contains a significant portion of single stranded regions. Common substructures were found in each predicted structure such as similar hairpin loops, duplexed, and linear regions such as the 18 nucleotide substructure (Su18). More specifically, a 32 nucleotide hairpin substructure (Su32), found near the 5' end, is present in each structure (Figure 3). The pervasiveness of this substructure is suggestive of its stability.

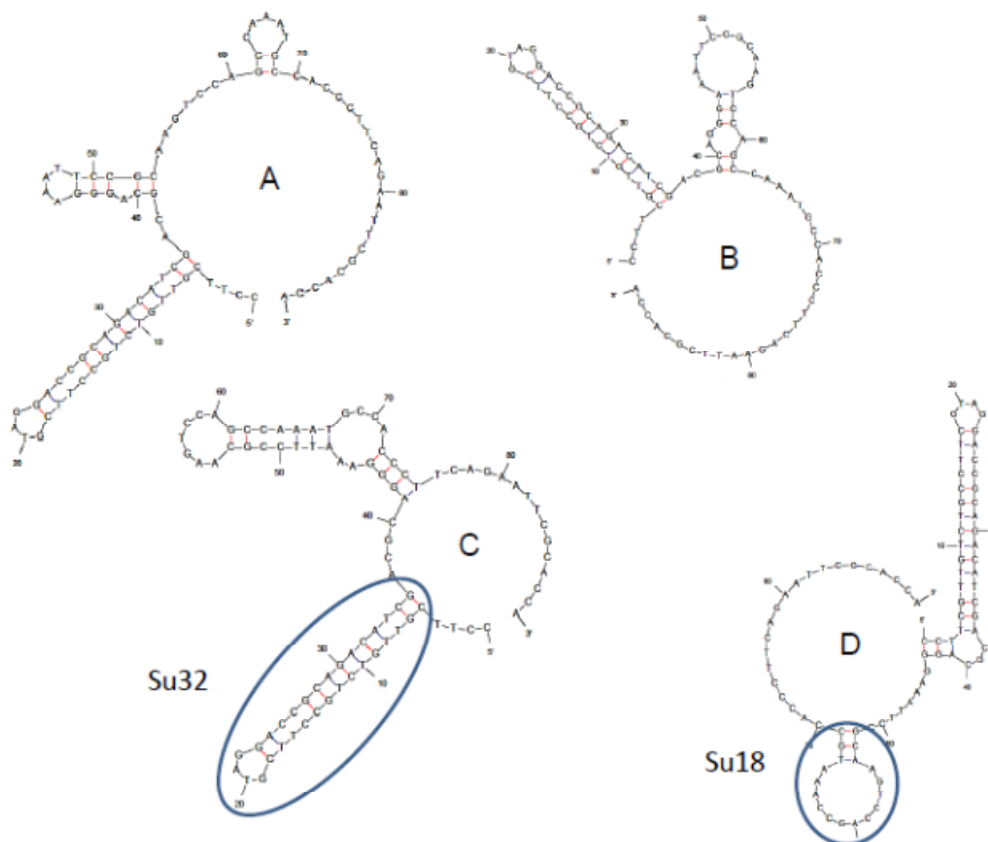


**Figure 3:** MFOLD secondary structure predictions of Ap90. The software MFOLD generated secondary structures for the aptamer with similar energies of  $-9.15$  kcal/mol (A),  $-9.12$  kcal/mol (B),  $-9.13$  kcal/mol (C), and  $-8.89$  kcal/mol (D). The circled substructures in prediction C and D are Su32 and Su18, the substructures that were synthesized and compared to Ap90 via NMR.

***Aptamer Structure by NMR:*** Most NMR structures of nucleic acids are of relatively small and well structured sequences while larger oligonucleotides ( $>30$  nt) generally require isotopic labeling<sup>17</sup>. Ap90 is not labeled and apparently contains segments of unstructured region; however, NMR can still be applied to identify base pairing. Each base pair gives rise to an imino proton peak in a characteristic chemical shift window (Figure 4). This peak is due to the fact that the imino proton is engaged in hydrogen bonding with the base pair partner and therefore does not exchange readily with water<sup>17</sup>. The slower the exchange with water the sharper the peak; base pairs at the end of a helix are more exposed resulting in broader peaks. Similarly, raising the temperature results in denaturation of the DNA duplex and causes the disappearance of the imino proton

resonance. Imino proton peaks show up very far downfield in the 12-14ppm range isolating them from the majority of the other peaks which would otherwise overcrowd the spectra<sup>17</sup>. Typically, GC base pairs resonate around 12 ppm and AT base pairs are near 14 ppm, this makes it possible to estimate the number of base pairs formed in the DNA duplex (Figure 4)<sup>18</sup>. Thus NMR can be a tool to determine base pair formation in solution and observe variation due to temperature (DNA melting) or solution conditions (salt, counterions, pH). A prerequisite for recording imino proton NMR spectra is that the samples are dissolved in water rather than D<sub>2</sub>O because imino protons exchange readily with D<sub>2</sub>O making them invisible. The robust jump and return pulse sequence was used for solvent suppression, where the delays and pulses are applied to avoid producing a water signal<sup>17</sup>.

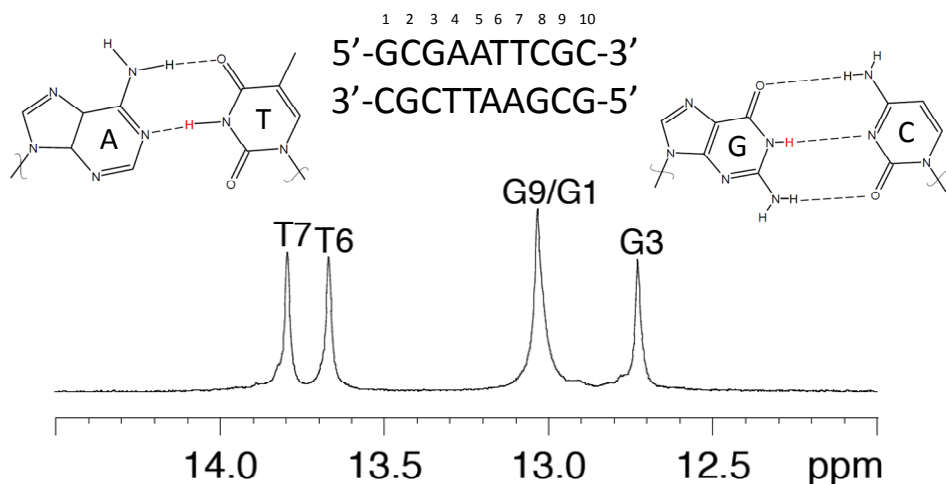


**Figure 4:** NMR spectrum of the palindromic 10-mer GCGAATTCGC (2.6mM). The conditions of the sample were 90% D<sub>2</sub>O, 50mM NaCl, 10mM sodium phosphate buffer, pH 6.5, at 293K<sup>18</sup>. The sequence has 10 base pairs, although given the molecules symmetry, only 5 of its base pairs are unique giving rise to the 5 peaks shown in the spectrum.

In order to examine the number and location of base paired structures present in Ap90, <sup>1</sup>H NMR spectra were recorded under low salt conditions (50mM) at low (15° C) and high temperatures (35° C). The spectra demonstrate that the aptamer was only forming about 7-8 base pairs (Figure 5) with more base pairs ~11 at lower temperature. At 15° C two additional imino proton resonances appear near 10.5ppm that likely originate from G and T nucleotides located in a hairpin loop. Increasing the temperature to 55° C results in loss of base pairs and

at 65° C no imino proton resonances could be detected. Since the extent of base pairing is dependent on external factors such as salt concentration and temperature, additional spectra were recorded under a wide array of conditions. Increasing the salt concentrations will help stabilize secondary and tertiary structures of DNA by reducing electrostatic repulsion of the negatively charged phosphodiester groups. Both monovalent (300mM NaCl) and divalent (4mM MgCl<sub>2</sub>) salts were investigated in tris- and sodium phosphate buffer solutions (Figure 6). However, the spectra revealed that the higher salt conditions and different buffers did little to stabilize the structure as no additional base pairs were formed.

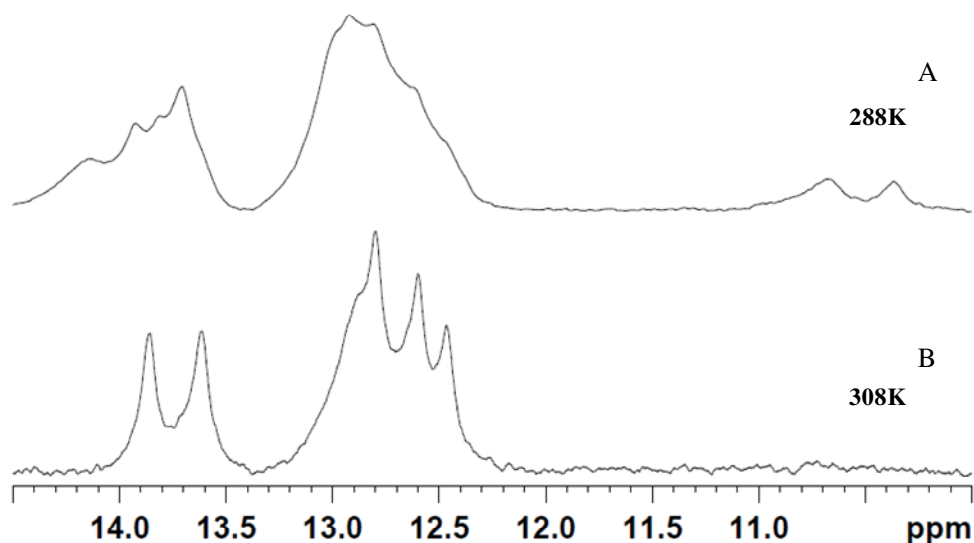


**Figure 5:** <sup>1</sup>H NMR Spectra of Ap90 with varying temperatures. Spectra A and B show the aptamer (0.5mM) at 288K and 308K respectively. The sample was dissolved in 10mM sodium phosphate buffer with 50mM NaCl, 1.4mM EDTA, and 10% D<sub>2</sub>O/ 90% H<sub>2</sub>O. The lower temperature slows down the solvent exchange, stabilizing a few weak base pairs.

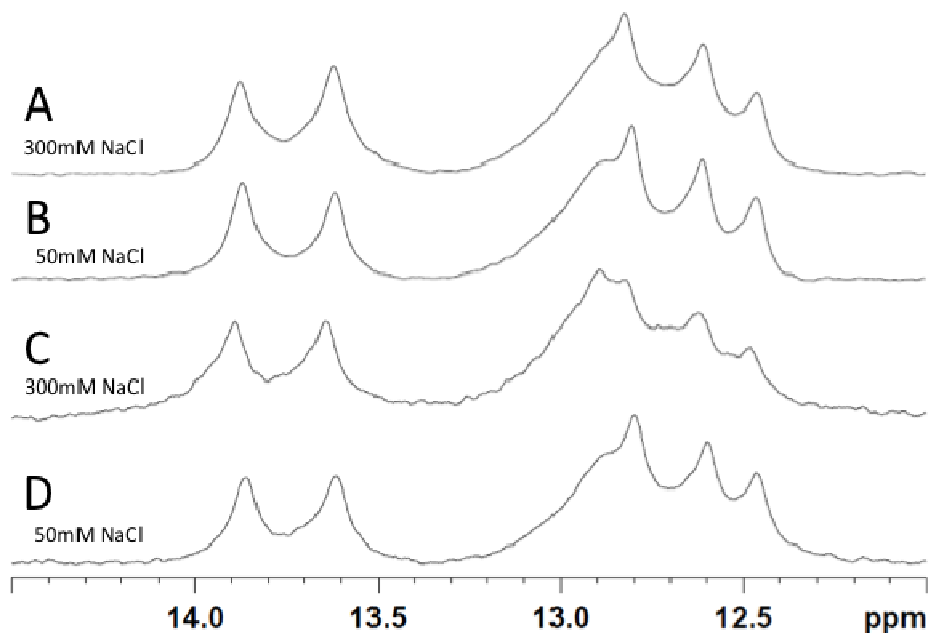


**Figure 6:**  $^1\text{H}$  NMR Spectra of Ap90 under various buffer and salt conditions. Spectra A and B compare Ap90 with tris buffer (pH 7.3) with NaCl conditions of 300mM and 50mM respectively. Spectra C and D compare the aptamer with sodium phosphate buffer (pH 7.0) with NaCl conditions of 300mM and 50mM respectively. Spectra were measured at 308K each with 1.4mM EDTA, 4mM  $\text{MgCl}_2$  and 0.5mM Ap90 in 10%  $\text{D}_2\text{O}$  / 90%  $\text{H}_2\text{O}$ .

In addition to the existence and number of base pairs formed in Ap90 NMR can also provide the location of the base paired regions in the aptamer. However the large size of the aptamer coupled with low concentration samples render standard assignment techniques impractical. To overcome this, the imino proton fingerprint of isolated substructures can be compared with the imino proton spectra of the full-length aptamer to determine which substructures are present in Ap90. To test this hypothesis, 2 substructures, predicted by the program MFOLD, were selected and examined for base pair formation by NMR under similar conditions as Ap90. The 18-mer substructure, Su18, predicted in several MFOLD structures (Figure 3) did not show any imino proton resonances in 50mM NaCl solutions at 25°C, demonstrating that this substructure is not stable. In contrast, a larger 32 nucleotide substructure, Su32, showed a remarkably similar base pair pattern as Ap90 (Figure 7). Minor differences in the spectra can be attributed to the reduced stability of the GC base pair at the base of the hairpin, which lacks the support of the rest of the molecule that Ap90 has. When the temperature was dropped to 15 °C two additional peaks appeared

~10.5ppm similar to the full-length aptamer, these resonances likely arise from G and T nucleotides in the hairpin loop.

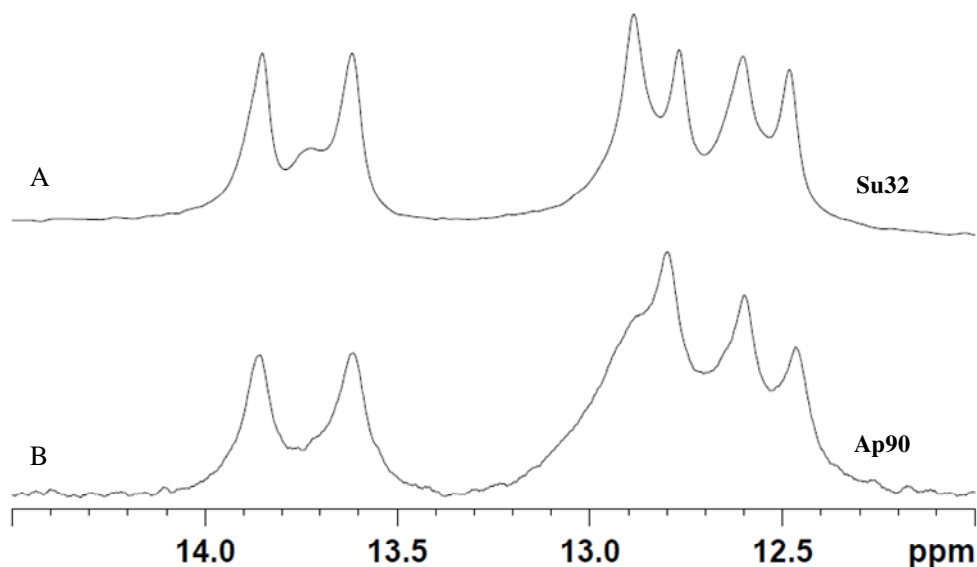


**Figure 7:**  $^1\text{H}$  NMR Spectra of the 32-mer Primer Region (A) and Ap90 (B). The spectra were collected at 308K, 50mM NaCl, sodium phosphate buffer (pH 7.0), and 1.4mM EDTA with 0.5mM Ap90.

Su32 can form a maximum of 4 AT and 7 GC base pairs (Figure 8). This number is consistent with the NMR spectra of Ap90 and Su32 at 15°C where 4-5 AT and 6-8 GC base pairs are estimated. At higher temperatures less stable regions containing only a few base pairs denature and their NMR signal disappears. At 35 °C, 2-3 AT and 4-5 GC base pairs are observed. This corresponds to the more stable 7 base pair duplex region underlined in figure 8.

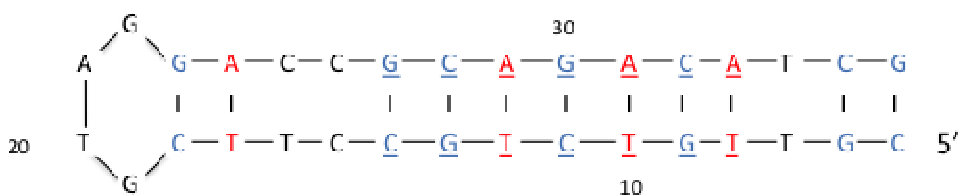


**Figure 8:** Hairpin structure of Su32. The AT base pairs are shown in red while the GC base pairs are in blue. The more stable base pairs are underlined and are responsible for the peaks in the NMR spectra at 35°C. The numbers annotate the position of the nucleotides relative to Ap90.

In an attempt to mimic some of the effect of the carbohydrates that are present on fibrinogen, the aptamers target, sucrose was added to Ap90. Even at a large excess of the disaccharide (0.1M sucrose, 160  $\mu$ M Ap90, 50mM NaCl, 10mM sodium phosphate buffer, and 1.4mM EDTA at 25°C) no additional base pairs were observed (Figure 9). However, fibrinogen contains branched oligosaccharides that are attached at defined positions on the protein<sup>19</sup>. Therefore complex carbohydrates might be more appropriate although they still lack the correct spatial arrangement present on fibrinogen.

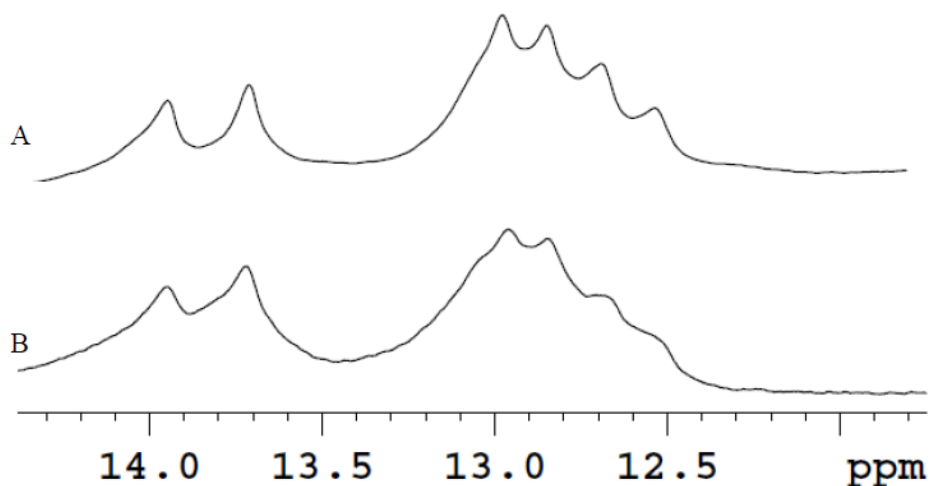


**Figure 9:** (A) Ap90 with 0.1M Sucrose. (B) Ap90 without sucrose. Both samples are shown at 298K with 50mM NaCl, 10mM sodium phosphate, 1.4mM EDTA pH 7.0.

### **Conclusion**

Native gel electrophoresis demonstrated that the 90mer aptamer Ap90 is partially folded as evidenced from its unusual mobility. The native gel also indicated that the aptamer can adopt many conformations because the band of Ap90 corresponds to a large variation in size. Both of these observations are consistent with the results from MFOLD which predicted a number of structures with similar energies that all contained a similar extent of base paired regions. NMR studies showed that Ap90, despite its size, only forms a few stable base pairs. At higher temperatures only 2-3 AT and 5-6 GC base pairs could be

detected. Lowering the temperature produces a total of 4-5 AT and 6-8 GC base pair. The extent of base pairing was unaffected to changes in the buffer conditions as high and low salt samples as well as samples containing  $Mg^{2+}$  did not significantly change the spectrum. The base paired region of Ap90 was identified by comparing imino proton spectra of substructures (Su18 and Su32) that occurred frequently in the MFOLD predictions. This identified a segment, corresponding to Su32, located near the 5' primer region from nucleotides 5-36 as the only base paired region. Based on this work Ap90, with exception of the primer region, is not involved in stable base pairing indicating a largely unstructured free aptamer. This is in agreement with the gel electrophoresis data which provided evidence of a large number of possible conformations. Taken together this suggests that the free aptamer does not contain a preexisting binding motif but rather will assume a structure upon interaction with its target. These results provide additional design parameters, namely the investigation of the role of the primer region. Is this region directly involved in binding or is it necessary to restrict the flexibility of portions of the aptamers. This provides a rational approach to dissect and understand the roles of different portions of the aptamer for fibrinogen binding and will aid the design of more efficient aptamers.

## References

- 1) Robertson, D. L., Joyce, G. F. (1990) Selection in vitro of an RNA enzyme that specifically cleaves single-stranded DNA *Nature* 344, 467–468.
- 2) Ellington, A. D., Szostak, J.W. (1990) In vitro selection of RNA molecules that bind specific ligands *Nature* 346, 818–822.
- 3) Tuerk, C., Gold, L. (1990) Systematic evolution of ligands by exponential enrichment: RNA ligands to bacteriophage T4 DNA polymerase *Science* 249, 505–510.
- 4) Zimmermann, G. R., Wick C. L., Shields T. P., Jenison R. D., Pardi A. (2000) Molecular interactions and metal binding in the theophylline-binding core of an RNA aptamer *RNA* 6, 659–667.
- 5) Jeon, S. H., Kayhan, B. Ben-Yedidia, T., Arnon R. (2004) A DNA aptamer prevents influenza infection by blocking the receptor binding region of the viral hemagglutinin *J. Biol. Chem.* 279, 48410-48419.
- 6) Romig, T. S., Bell, C., Drolet, D. W. (1999) Aptamer affinity chromatography: combinatorial chemistry applied to protein purification *Journal of Chromatography* 731, 275-284.

- 7) Kleinjung, F., Klussmann, S., Erdmann, V. A., Scheller, F. W., Fürste, J. P., Bier, F. F. (1998) High-affinity RNA as a recognition element in a biosensor *Anal. Chem.* 70 328-331.
- 8) Nimjee, S. M., Rusconi, C. P., Sullenger, B. A. (2005) Aptamers: an emerging class of therapeutics *Annu Rev Med* 56, 555-583.
- 9) Brody, E. N., Gold, L. (2000) Aptamers as therapeutic and diagnostic agents *J. Biotech.* 74, 5-13.
- 10) Pegaptanib injection.  
<http://www.ncbi.nlm.nih.gov/pubmedhealth/PMH0000406/> (accessed 7-22-2011).
- 11) Dey, A. K., Griffiths, C., Lea, S. M., James, W. (2005) Structural characterization of an anti-gp120 RNA aptamer that neutralizes R5 strains of HIV-1 *RNA* 11, 873-884.
- 12) Macaya, R. F., Schultze, P., Smith, F. W., Roe, J. A., Feigon, J. (1993) Thrombin-binding DNA aptamer forms a unimolecular quadruplex structure in solution *PNAS* 90, 3745-3749.
- 13) Li, M., Lin, N., Huang, Z., Du, L., Altier, C., Fang, H., Wang, B. (2008) Selecting aptamers for a glycoprotein through the incorporation of the boronic acid moiety *J. Am. Chem. Soc.* 130, 12636-12638.
- 14) (2002) Applied biosystems manual for 391 DNA synthesizer.
- 15) Germann, M. W. (1989) Ph.D. Thesis, The University of Calgary.
- 16) Zuker, M. The mfold Web Server.  
<http://mfold.rna.albany.edu/?q=mfold/DNA-Folding-Form> (accessed 7-22-2011).
- 17) Plateau, P., Gueron, M. (1982) Exchangeable proton NMR without base-line distortion, using new strong-pulse sequence *J. Am. Chem. Soc.* 104, 7310-7311.
- 18) Aramini, J. M., Kalisch, B. W., Pon, R. T., van de Sande, J. H., Germann, M. W. (1996) Structure of a DNA duplex that contains  $\alpha$ -anomeric nucleotides and 3'-3' and 5'-5' phosphodiester linkages: Coexistence of parallel and antiparallel DNA *Biochemistry* 35, 9355-9365.
- 19) Townsend, R. R., Hilliker, E., Li, Y., Laine, R. A., Bell, W. R., Lee, Y. C. (1982) Carbohydrate Structure of Human Fibrinogen *J. Biol. Chem.* 257, 9704-9710